THE ASTROPHYSICAL JOURNAL, 428:275–283, 1994 June 10

GRAVITATIONAL INSTABILITIES IN A PROTO-PLANETARY DISK INCLUDING THE EFFECTS OF MAGNETIC FIELDS

HYERIM NOH,[1] ETHAN T. VISHNIAC, AND WILLIAM D. COCHRAN
University of Texas, Austin, TX 78712
E-mail: ethan@astro.as.utexas.edu, wdc@astro.as.utexas.edu
Received 1991 August 8; accepted 1993 November 19

ABSTRACT

We investigate the gravitational instability of a thin, Keplerian protoplanetary disk including the effects of a largely azimuthal magnetic field. The model follows that of our previous work (Noh, Vishniac, & Cochran 1991) except for the inclusion of a magnetic field. The disk is assumed to consist of neutral and ionized gas and neutral dust which are coupled by gravity and friction. The growth rates and eigenfunctions are calculated numerically using nonaxisymmetric linear perturbation methods. The results show that the growth rate has a maximum at some intermediate azimuthal number m, but for each value of m it is reduced relative to the unmagnetized case. The effects of the magnetic field appear more strongly on small scales. As the strength of the equilibrium magnetic field increases the growth rates decrease, and the maximum instability occurs at a lower value of m due to the increasing magnetic pressure. The response of each component to the magnetic field is discussed using the behavior of the eigenfunctions in the radial direction. With the inclusion of the magnetic field, the effects of the ionization fraction and friction on the growth rates also appear to be important for high m modes. Increasing the ionization fraction or the friction suppresses instability, but only slightly changes the maximally unstable azimuthal scales. The enhanced growth rates due to a dust component for which thermal pressure is negligible are somewhat reduced by the inclusion of a magnetic field. The effects of different boundary conditions (reflecting and transmitting) on the growth rates are also shown.

Subject headings: instabilities — MHD — planets and satellites: general — stars: formation

1. INTRODUCTION

Strong evidence for the existence of disks around young stellar objects and pre–main-sequence stars based on the IR and UV observations (Aumann et al. 1984; Bertout, Basri, & Bouvier 1988; Strom et al. 1989) has stimulated interest in the investigation of star or planetary formation in such disks. Gravitational instability is one of the mechanisms which may lead to star or planet formation and recently several attempts have been made to explain the observational properties of these disks using the nonaxisymmetric normal mode perturbation methods (Larson 1984; Papaloizou, & Lin 1989; Adams, Ruden, & Shu 1989; Shu et al. 1990).

In a previous paper by Noh, Vishniac, & Cochran (1991, hereafter NVC), we discussed the stability of a thin, Keplerian protoplanetary disk which consists of gas and dust. The main result is that there are some intermediate scales in both the azimuthal and radial direction which are gravitationally unstable, and the fastest growing modes correspond to the growing "lumps." Also, the instability of the disk increases with the inclusion of dust for which the pressure is negligible, although the dust is only a small fraction, by mass, of the disk.

The purpose of this paper is to extend this work by including a global magnetic field. We will discuss the evolution of nonaxisymmetric linear perturbations in a Keplerian, magnetic disk consisting of gas and dust. Here we just assume the existence of a strong field without regard to its dynamics.

A magnetic field can play an important role in instabilities in a disk with even a slight degree of ionization if it is strongly coupled to the disk material. In particular a nonaxisymmetric perturbation in a shearing disk can be strongly influenced by the magnetic field, i.e., the perturbation can be twisted by Coriolis forces, while magnetic tension resists the Coriolis force and allows the perturbation to lose angular momentum (Elmegreen 1987). We will examine the effect of a magnetic field on the growth rates for each azimuthal number m. Our study is concentrated on high m modes using high numerical resolution. Instead of using two fluids (e.g., gas and dust) in NVC, we treat the disk as a three fluid system, consisting of the ionized gas, neutral gas, and neutral dust. We assume that these components are coupled by the gravity and the friction. We describe the equilibrium model and the linearized equations with the boundary conditions in § 2. In § 3, the numerical methods are given. In § 4, the results are presented and also the discussions are given.

2. MODEL DESCRIPTION

2.1. *Equilibrium*

Our model follows that of NVC except for the inclusion of a magnetic field. First, we briefly summarize the previous model. We consider geometrically thin ($H/R \ll 1$), and Keplerian disk ($\Omega \propto r^{-3/2}$), where H is the half thickness of the disk, R is the radius of the disk, and Ω is the angular frequency. We use cylindrical coordinates (r, ϕ, z), where r is the radial direction, ϕ is the azimuthal direction, and z is the direction perpendicular to the disk. In a thin disk limit, the equations are vertically averaged, so the system becomes two-dimensional. We take the velocities in equilibrium as $v_{0r} = 0$, $v_{0\phi} = r\Omega(r)$, $v_{0z} = 0$. The equilibrium surface density and temperature distributions are taken from Adams et al. (1989) in which all quantities are power laws in $r[\sigma_{0*} r^{-p}$, $T = T_{0*} r^{-q} (c_s = c_{s0*} r^{-q/2})$, where σ_{0*}, T_{0*}, c_{s0*}, p, and q are constants].

[1] Currently at Korea National Observatory, San 36-1, Whaam-dong, Yusung-gu, Daejon, Korea. E-mail: hr@apissa.issa.re.kr

In this paper the disk is a three fluid system, consisting of ionized gas, neutral gas and neutral dust. Since dust is only a small fraction of the total mass, the effect of the ionized dust on the results may be small unless pressureless dust can initiate gravitational instabilities. As in NVC, the dust and gas are coupled by gravity and friction. Here, since there are three components, we need three different friction coefficients, i.e., $A_{\rm gn,gi}$, $A_{\rm gn,dn}$, and $A_{\rm gi,dn}$, where the subscripts gn, gi, and dn denote neutral gas, ionized gas, and neutral dust component, respectively. In order to describe the system, we need the basic magnetohydrodynamic equations, i.e., conservation of mass, momentum, magnetic induction equation, and Poisson's equation. In the following equations, we denote the equilibrium and perturbed state by the subscripts 0 and 1, respectively.

The continuity equations for the ionized and neutral gas and neutral dust are

$$\frac{\partial \sigma_{\rm gi,gn,dn}}{\partial t} + \nabla \cdot (\sigma_{\rm gi,gn,dn} \boldsymbol{v}_{\rm gi,gn,dn}) = 0 , \tag{2.1}$$

where, $\sigma_{\rm gi,gn,dn}$ are the surface densities of the ionized, neutral gas, and neutral dust components and $\boldsymbol{v}_{\rm gi,gn,dn}$ are their velocities.

The equations of motion of gas and dust are

$$\sigma_{\rm gi}\frac{\partial \boldsymbol{v}_{\rm gi}}{\partial t} + \sigma_{\rm gi}(\boldsymbol{v}_{\rm gi}\cdot\nabla)\boldsymbol{v}_{\rm gi} = -\sigma_{\rm gi}\nabla\Phi - \nabla p_{\rm gi} + \frac{1}{4\pi} \times \int_{-\infty}^{\infty} dz[(\nabla \times \boldsymbol{B}) \times \boldsymbol{B}] - \boldsymbol{f}_{\rm gi,gn} - \boldsymbol{f}_{\rm gi,dn} , \tag{2.2}$$

$$\sigma_{\rm gn}\frac{\partial \boldsymbol{v}_{\rm gn}}{\partial t} + \sigma_{\rm gn}(\boldsymbol{v}_{\rm gn}\cdot\nabla)\boldsymbol{v}_{\rm gn} = -\sigma_{\rm gn}\nabla\Phi - \nabla p_{\rm gn} - \boldsymbol{f}_{\rm gn,gi} - \boldsymbol{f}_{\rm gn,dn} , \tag{2.3}$$

$$\sigma_{\rm dn}\frac{\partial \boldsymbol{v}_{\rm dn}}{\partial t} + \sigma_{\rm dn}(\boldsymbol{v}_{\rm dn}\cdot\nabla)\boldsymbol{v}_{\rm dn} = -\sigma_{\rm dn}\nabla\Phi - \boldsymbol{f}_{\rm dn,gn} - \boldsymbol{f}_{\rm dn,gi} , \tag{2.4}$$

where Φ is the gravitational potential, $p_{\rm gi,gn}$ is the pressure of the ionized and neutral gas, We assume that the pressure is negligible for the dust. The quantity $\boldsymbol{f}_{\rm gi,gn}$ is the friction force between ionized and neutral gas and is assumed to be proportional to the relative velocity between two components

$$\boldsymbol{f}_{\rm gi,gn} = A_{\rm gi,gn}\sigma_{\rm gi}\sigma_{\rm gn}(\boldsymbol{v}_{\rm gi} - \boldsymbol{v}_{\rm gn}) , \tag{2.5}$$

where $\boldsymbol{f}_{\rm gi,gn} = -\boldsymbol{f}_{\rm gn,gi}$. The quantity A is the friction coefficient and is defined as

$$A_{\rm gi,gn} = \langle \sigma v \rangle_{\rm gi,gn}/(m_{\rm gi} + m_{\rm gn}) ,$$

where $\langle \sigma v \rangle_{\rm gi,gn}$ is the average collision rate between ionized and neutral gas with mass $m_{\rm gi}$ and $m_{\rm gn}$, respectively (Spitzer 1978) and the same form applies to the other components.

The magnetic field interacts directly with the ionized gas by the Lorentz force. For the neutral gas and dust, the magnetic field is coupled indirectly by collisions with the ionized component. The dust will be ionized, but since the charge to mass ratio will be very small, the Lorentz force on the dust will be negligible. Therefore, the effect of the magnetic field on the system in which the neutral gas dominates is sensitive to the strength of the coupling to the ionized component. In this paper, we assume that the fluid is highly conducting in the sense that ohmic dissipation is negligible. We will return to this point in § 4.2. We assume that the gas is only slightly ionized, and the magnetic field moves with the ionized gas. The magnetic induction equation is

$$\frac{\partial \boldsymbol{B}}{\partial t} = \nabla \times (\boldsymbol{v}_{\rm gi} \times \boldsymbol{B}) . \tag{2.6}$$

The equilibrium magnetic field components B_{0r}, $B_{0\phi}$ are assumed to depend on the radial distance ($\propto r^{-1}$) so that the magnetic pressure has the same radial dependence as the gas pressure and the inclination of the field lines does not vary with radius. In general we can assume that B_{0z} is negligible compared with other field components since for a thin disk ($H/r \ll 1$)$\nabla \cdot \boldsymbol{B} = 0$ implies $B_{0z} \sim (H/r)B_{0r}$. In this particular case we have taken $B_{0r} \propto r^{-1}$ so that $\nabla \cdot \boldsymbol{B} = 0$ for $B_{0z} = 0$. Also, given the strong effect of shearing we take $B_{0\phi} \gg B_{0r}$. More realistically, this ratio is fixed by a balance between dissipation and some dynamo mechanism. Here we neglect this aspect of the disk dynamics, the details of any dynamo being highly uncertain at best, and simply assume this ratio is large enough that the radial magnetic field has a small effect on the dynamics.

Poisson's equation for these three fluids is given by

$$\nabla^2\Phi = 4\pi G(\sigma_{\rm gn} + \sigma_{\rm gi} + \sigma_{\rm dn})\delta(z) . \tag{2.7}$$

2.2. *Perturbed Equations*

As in NVC, we consider normal mode perturbations of the form

$$\sigma_1 = \sigma_1(r)e^{i(wt - m\phi)} , \tag{2.8}$$

where m is the azimuthal number, w is the frequency, and $\sigma_1(r)$ is the radial component of the perturbed surface density. For other variables ($\boldsymbol{v}$, $\boldsymbol{B}$, p, Φ), we use the same perturbation forms. The eignevalue and the variables are the complex numbers. The real component w_R of the eigenvalue w gives the phase velocity, and the imaginary component w_I gives the growth rate. For an unstable system, w_I must be negative. In order to make these equations dimensionless, we adopt the following variables:

$$\tilde{\boldsymbol{v}}_1 = \frac{\boldsymbol{v}_1}{r_D\Omega_D} , \quad \tilde{\Phi}_1 = \frac{\Phi_1}{(r_D\Omega_D)^2} , \quad \tilde{\sigma}_1 = \frac{\sigma_1}{\sigma_0} , \quad \tilde{w} = \frac{w}{\Omega_D} ,$$
$$\tilde{\Omega} = \frac{\Omega}{\Omega_D} , \quad \tilde{r} = \frac{r}{r_D} , \quad \tilde{h}_1 = \frac{h_1}{(r_D\Omega_D)^2} , \quad \tilde{A} = \frac{A}{\Omega_D\sigma_o^{-1}} , \tag{2.9}$$
$$\tilde{\boldsymbol{B}} = \frac{\boldsymbol{B}}{r_D\Omega_D\sigma_{\rm gi0}^{1/2}H^{-1/2}} ,$$

where r_D, and Ω_D are the disk radius, and the angular velocity at r_D, respectively. Substituting the perturbed forms into the equations in § 2.1 and using these dimensionless variables, we obtain the following equations for the ionized and neutral gas and the neutral dust.

Continuity equation:

$$\frac{d\tilde{v}_{\rm gi1r,gn1r,dn1r}}{d\tilde{r}} = \frac{p-1}{\tilde{r}}\tilde{v}_{\rm gi1r,gn1r,dn1r} + \frac{im}{\tilde{r}}\tilde{v}_{\rm gi1\phi,gn1\phi,dn1\phi} - i(\tilde{w} - m\tilde{\Omega})\tilde{\sigma}_{\rm gi1,gn1,dn1} . \tag{2.10}$$

Equation of motion:

r component:

$$i(\tilde{w}-m\tilde{\Omega})\tilde{v}_{\mathrm{gn1}r}-2\tilde{\Omega}\tilde{v}_{\mathrm{gn1}\phi}=-\frac{d}{d\tilde{r}}(\tilde{\Phi}_1+\tilde{h}_{\mathrm{gn1}})-\tilde{A}_{\mathrm{gn,gi}}(\tilde{v}_{\mathrm{gn1}r}-\tilde{v}_{\mathrm{gi1}r})-\tilde{A}_{\mathrm{gn,dn}}(\tilde{v}_{\mathrm{gn1}r}-\tilde{v}_{\mathrm{dn1}r}), \quad (2.11)$$

$$i(\tilde{w}-m\tilde{\Omega})\tilde{v}_{\mathrm{gi1}r}-2\tilde{\Omega}\tilde{v}_{\mathrm{gi1}\phi}=-\frac{d}{d\tilde{r}}(\tilde{\Phi}_1+\tilde{h}_{\mathrm{gi1}})+\frac{1}{2\pi}\times\left[-\tilde{B}_{0\phi}\frac{d\tilde{B}_{1\phi}}{d\tilde{r}}-\frac{2\tilde{B}_{0\phi}}{\tilde{r}}\times\tilde{B}_{1\phi}-\frac{im\tilde{B}_{0\phi}}{\tilde{r}}\tilde{B}_{1r}+\tilde{\sigma}_{\mathrm{gi1}}\frac{\tilde{B}_{0\phi}^2}{\tilde{r}}-\tilde{B}_{1\phi}\frac{d\tilde{B}_{0\phi}}{d\tilde{r}}+\tilde{\sigma}_{\mathrm{gi1}}\tilde{B}_{0\phi}\frac{d\tilde{B}_{0\phi}}{d\tilde{r}}\right]-\tilde{A}_{\mathrm{gi,gn}}(\tilde{v}_{\mathrm{gi1}r}-\tilde{v}_{\mathrm{gn1}r})-\tilde{A}_{\mathrm{gi,dn}}(\tilde{v}_{\mathrm{gi1}r}-\tilde{v}_{\mathrm{dn1}r}), \quad (2.12)$$

$$i(\tilde{w}-m\tilde{\Omega})\tilde{v}_{\mathrm{dn1}r}-2\tilde{\Omega}\tilde{v}_{\mathrm{dn1}\phi}=-\frac{d}{d\tilde{r}}\tilde{\Phi}_1-\tilde{A}_{\mathrm{dn,gn}}(\tilde{v}_{\mathrm{dn1}r}-\tilde{v}_{\mathrm{gn1}r})-\tilde{A}_{\mathrm{dn,gi}}(\tilde{v}_{\mathrm{dn1}r}-\tilde{v}_{\mathrm{gi1}r}). \quad (2.13)$$

ϕ component:

$$\frac{1}{2}\tilde{\Omega}\tilde{v}_{\mathrm{gn1}r}+i(\tilde{w}-m\tilde{\Omega})\tilde{v}_{\mathrm{gn1}\phi}=\frac{im}{\tilde{r}}(\tilde{\Phi}_1+\tilde{h}_{\mathrm{gn1}})-\tilde{A}_{\mathrm{gn,gi}}(\tilde{v}_{\mathrm{gn1}\phi}-\tilde{v}_{\mathrm{gi1}\phi})-\tilde{A}_{\mathrm{gn,dn}}(\tilde{v}_{\mathrm{gn1}\phi}-\tilde{v}_{\mathrm{dn1}\phi}), \quad (2.14)$$

$$\frac{1}{2}\tilde{\Omega}\tilde{v}_{\mathrm{gi1}r}+i(\tilde{w}-m\tilde{\Omega})\tilde{v}_{\mathrm{gi1}\phi}=\frac{im}{\tilde{r}}(\tilde{\Phi}_1+\tilde{h}_{\mathrm{gi1}})+\frac{1}{2\pi}\times\left[\tilde{B}_{0r}\frac{d\tilde{B}_{1\phi}}{d\tilde{r}}+\frac{\tilde{B}_{0r}}{\tilde{r}}\tilde{B}_{1\phi}+\left(\frac{\tilde{B}_{0\phi}}{\tilde{r}}+\frac{\tilde{B}_{0r}im}{\tilde{r}}\right)\tilde{B}_{1r}-\tilde{\sigma}_{\mathrm{gi1}}\frac{\tilde{B}_{0r}\tilde{B}_{0\phi}}{\tilde{r}}+\tilde{B}_{1r}\frac{d\tilde{B}_{0\phi}}{d\tilde{r}}-\tilde{\sigma}_{\mathrm{gi1}}\tilde{B}_{0r}\frac{d\tilde{B}_{0\phi}}{d\tilde{r}}\right]-\tilde{A}_{\mathrm{gi,gn}}(\tilde{v}_{\mathrm{gi1}\phi}-\tilde{v}_{\mathrm{gn1}\phi})-\tilde{A}_{\mathrm{gi,dn}}(\tilde{v}_{\mathrm{gi1}\phi}-\tilde{v}_{\mathrm{dn1}\phi}), \quad (2.15)$$

$$\frac{1}{2}\tilde{\Omega}\tilde{v}_{\mathrm{dn1}r}+i(\tilde{w}-m\tilde{\Omega})\tilde{v}_{\mathrm{dn1}\phi}=\frac{im}{\tilde{r}}\tilde{\Phi}_1-\tilde{A}_{\mathrm{dn,gn}}(\tilde{v}_{\mathrm{dn1}\phi}-\tilde{v}_{\mathrm{gn1}\phi})-\tilde{A}_{\mathrm{dn,gi}}(\tilde{v}_{\mathrm{dn1}\phi}-\tilde{v}_{\mathrm{gi1}\phi}), \quad (2.16)$$

where the perturbed enthalpy of the ionized and neutral gas $h_{\mathrm{gi1,gn1}}$ on the adiabatic assumption is defined

$$h_{\mathrm{gi1,gn1}}\equiv c_{\mathrm{gs}}^2\sigma_{\mathrm{gi1,gn1}}/\sigma_{\mathrm{gi0,gn0}}. \quad (2.17)$$

Also, we used the epicyclic frequency $\kappa=\Omega$ for a Keplerian disk, where

$$\kappa^2\equiv\frac{1}{r^3}\frac{d}{dr}[(r^2\Omega)^2]. \quad (2.18)$$

Induction equation:

$$\left(-\frac{\tilde{B}_{0r}}{\tilde{r}}-\frac{im\tilde{B}_{0\phi}}{\tilde{r}}-\frac{d\tilde{B}_{0r}}{d\tilde{r}}\right)\tilde{v}_{\mathrm{gi1}r}+\frac{im\tilde{B}_{0r}}{\tilde{r}}\tilde{v}_{\mathrm{gi1}\phi}-i(\tilde{w}-m\tilde{\Omega})\tilde{B}_{1r}=0, \quad (2.19)$$

$$\left(-\tilde{B}_{0\phi}\frac{d}{d\tilde{r}}-\frac{d\tilde{B}_{0\phi}}{d\tilde{r}}\right)\tilde{v}_{\mathrm{gi1}r}+\left(\tilde{B}_{0r}\frac{d}{d\tilde{r}}-\frac{\tilde{B}_{0r}}{\tilde{r}}\right)\times\tilde{v}_{\mathrm{gi1}\phi}-\frac{3\tilde{\Omega}}{2}\tilde{B}_{1r}+i(m\tilde{\Omega}-\tilde{w})\tilde{B}_{1\phi}=0. \quad (2.20)$$

We note that $\nabla\cdot\boldsymbol{B}_1=0$ is implied by these perturbation equations. Poisson's equation:

$$\Phi_1=-\frac{2\pi G}{\Omega_D^2}r_D^{-p-1}\tilde{r}^{-p+1}\int_0^\infty K_m(x)x^{-p}\times(\sigma_{\mathrm{dn0}*}\tilde{\sigma}_{\mathrm{dn1}}+\sigma_{\mathrm{gi0}*}\tilde{\sigma}_{\mathrm{gi1}}+\sigma_{\mathrm{gn0}*}\tilde{\sigma}_{\mathrm{gn1}})dx. \quad (2.21)$$

Equation of state:

$$\tilde{h}_{\mathrm{gi1,gn1}}=h_*\tilde{r}^{-q}\tilde{\sigma}_{\mathrm{gi1,gn1}},\quad h_*\equiv\frac{c_{\mathrm{gs}}^2}{\Omega_D^2}r_D^{-q-2}. \quad (2.22)$$

2.3. *Boundary Conditions*

For the outer boundary condition (BC), we assume that a constant pressure is given by the external medium at the outer boundary. Then the Lagrangian perturbation of the total pressure (sum of gas pressure and magnetic pressure) is zero. Considering that the outer boundary is also deformed by the perturbation, the following condition must be satisfied at $r=r_D+\delta re^{i(wt-m\phi)}$, where δr is a constant to be determined by $v_{1r}(r_D)=iw\,\delta r$. On the assumption of adiabatic perturbation, the outer BC to the linear order is

$$\Delta(p_g+p_{\mathrm{mag}})=\frac{c_{\mathrm{gs}}^2}{H}\left(\sigma_{g1}+\xi\frac{d\sigma_{g0}}{dr}\right)+\frac{B_0}{4\pi}\left(\boldsymbol{B}_1+\xi\frac{d\boldsymbol{B}_0}{dr}\right)=0, \quad (2.23)$$

where ξ is the Lagrangian displacement vector. Using the relation between ξ and the Lagrangian velocity perturbation Δv_{g1r} (Adams et al. 1989),

$$\left(\frac{\partial}{\partial t}+\Omega\frac{\partial}{\partial\theta}\right)\xi=\Delta v_{g1r}=v_{g1r}+\xi\cdot\nabla(\Omega r\hat{\theta}) \quad (2.24)$$

the outer BC can be rewritten as

$$\frac{c_{\mathrm{gs}}^2}{H}\left(\sigma_{g1}-\frac{iv_{g1r}}{w-m\Omega}\frac{d\sigma_{g0}}{dr}\right)+\frac{B_0}{4\pi}\left(\boldsymbol{B}_1-\frac{iv_{g1r}}{w-m\Omega}\frac{d\boldsymbol{B}_0}{dr}\right)=0. \quad (2.25)$$

Here we assumed that the disk thickness is a constant for a simplification. For a more physically reasonable BC we need to consider the effect of the perturbation on the disk thickness. The BC is usually important in determining an instability for the global modes. However, as we showed in NVC, for high m modes the effect of the BC on the growth rates appears small, i.e., even with the transmitting BC, the growth rates change only slightly.

The inner BC is much more complicated because of the difficult physical properties of central star and disk interface. As in NVC, we simply take two different BC; reflecting and transmitting BC. For the reflecting BC, we assume that the radial velocity of each component is zero at the inner boundary. For the transmitting BC, we assume that the perturbation propagates only inward (to the central star). Then for each

variable the following condition must be satisfied (i.e., $d\sigma_{gi1}/dr + i|k|\sigma_{gi1} = 0$). In principle, we can determine the radial wavenumber $|k|$ both numerically and analytically. Numerically, the wavenumber ($|k| = 2\pi/\lambda$) can be obtained from measuring the wavelength near the inner boundary. An analytical wavenumber can be obtained approximately from the WKBJ dispersion relation. However, in our system in which a magnetic field and friction effects are included for three components, the analytical dispersion relation turns out to be very complicated, and several simplifying assumptions are needed for an analysis. For this reason, here we use the numerically determined wavenumber rather than the analytical one. The importance and the effect of the BCs on the results will be discussed in § 4.2.

3. NUMERICAL METHODS

We use the same numerical iteration method as in NVC to solve the set of integrodifferential equations in § 2.2. Summarizing briefly the numerical method in NVC is the following; We used the Runge-Kutta method to integrate the system of the differential equations from inner to outer boundary, the Newton-Raphson method to find the eigenvalues w_R, w_I which satisfy BC, and the Simpson method for calculating the potential.

The difference between this work and NVC is that here we treat more components and magnetic field equations, so we have more variables (e.g., v_{gi1r}, $v_{gi1\phi}$, B_{1r}, $B_{1\phi}$) and equations. Since the effect of the magnetic field is more important in the inner region of the disk, we divide the disk radius into equally spaced zones in logarithmic intervals. The results vary somewhat depending on the numerical resolution, and we usually take 3000 grid points. Even when we increased the number of grid points up to 5000, the eigenvalues changed by less than 1%. Therefore our numerical resolution may be sufficient to calculate the growth rates. High m modes require higher resolution, and we increased the grid number up to 5000 for $m \geq 10$ modes. We iterated until the error range was less than 10^{-3} for finding the eigenvalue and also for the convergence of the variables and the potential. Typically, 8–9 iterations were required to obtain the converged solutions.

4. RESULTS AND DISCUSSION

4.1. *Parameters*

As in NVC, we choose the power law indices $p = 3/2$, $q = 1/2$ for the surface density and the temperature distribution in equilibrium. The temperature at the inner boundary is taken to be 3000 K following Adams et al. (1989). The masses of the central star and the disk are chosen to be 0.5 $M_\odot$, and the effect of the different mass of the disk on the instability will be shown. The ratio of the mass surface density of the neutral gas to that of the dust is 50 except as noted. The inner and outer disk radii are taken as 0.01 and 100 AU, respectively. In this paper, one of the new parameters is the ionization fraction x, the ratio of the equilibrium surface density of the ionized gas to that of the neutral gas. The fractional ionizations of the disks of young stellar objects are not well determined. Here we take a standard value of $x = 10^{-10}$, estimated from the relation between x and the number density n, i.e., x is proportional to $n^{-1/2}$ (Elmegreen 1979). In our disk n is large, i.e., near the outer edge of the disk, $n \sim 10^9$ cm^{-3}. The main sources of ionization are hydrogen ionizations by cosmic rays and radioactive elements (for temperatures less than several hundred kelvin and thermal ionization of alkali metals (for temperatures larger than several hundred K) (Umebayashi 1983; Umebayashi & Nakano 1988). In our model, we assume that the ionization balance is mainly determined by cosmic rays and take 10^{-17} s^{-1} as the ionization rate (Spitzer 1978), although thermal ionization might be important near the inner edge of the disk. However, the ionization balance also depends on several other poorly known factors. For example, ionization in the disk might be increased due to the decay of the ^{26}Al in the early solar nebula (Lee, Papanastassiou, & Wasserburg 1977), although this point is still controversial. Also, the ionization depends on the ratio of gas to dust, i.e., a larger ratio gives higher x (Umebayashi & Nakano 1988). This paper includes a comparison of results obtained with different values of x. Of course, in a realistic model of the protosolar nebula the ionization will be a function of radius and distance from the disk midplane. Our calculation is meant merely as an illustration of the effects of a magnetic field in a significantly conducting disk. In particular we note that the calculations of Umebayashi and Nakano indicate that the gas conductivity is very small from a radius of $\sim$15 AU to within a fraction of an astronomical unit (roughly comparable to the radius of Mercury's orbit). If these results are correct then our work should only be applied to perturbations at large and small radii. On the other hand, such a low ionization in the inner solar system makes it difficult to understand results of Levy & Sonett (1978) who found that carbonaceous chondrites show signs of cooling in a 1 G magnetic field, presumably at a solar radius of about 3 AU. Given the lack of chemical differentiation in such objects, this would seem to imply that the protosolar nebula was highly magnetized, or that cooling typically occurred in the neighborhood of some extreme field inhomogeneity, i.e., a strong flux tube or a hydromagnetic shock. Given these uncertainties, it seems worthwhile to explore the hypothesis that the protosolar nebula was uniformly strongly magnetized.

To determine the equilibrium magnetic field, we adopt the parameter $\beta^{-1} \equiv B_0^2 H/(2\pi\sigma_0 c_{gs}^2)$ which is the ratio of the magnetic pressure to the gas pressure in two dimensions. As mentioned earlier, we assume the azimuthal component of the magnetic field is much larger than the radial component ($B_{0\phi} = 100B_{0r}$) and they depend on the radial distance, i.e., $B_{0\phi,r} = B_{0\phi,r*}\, r^{-1}$. Then, the coefficients $B_{0\phi*}$, B_{0r*} are determined when β^{-1} is fixed. We have found that our results are insensitive to $B_{0r}/B_{0\phi}$ for values close to, or smaller than, the assumed ratio of 1:100. We show the effect of the magnetic field strength on the instability by varying the value of β^-. Also, we need to determine the friction coefficient A which depends on τ^{-1}, where τ is the collision timescale. We assume that the gas consists of mostly neutral hydrogen and a little amount of positive ions which have about the mass of carbon. We take $\langle\sigma v\rangle_{gn,gi} \sim 2.2 \times 10^{-9}$ cm^3 s^{-1}, $m_{dn} \sim 4 \times 10^{-14}$ g, $\rho_{dn} \sim 2$ g cm^{-3}, and $r_{dn} \sim 3 \times 10^{-5}$ cm (Spitzer 1978). We also vary the value of A and show the effect on our results.

4.2. *Results and Discussion*

In Figure 1, we show the growth rate ($\equiv -w_I$) for each azimuthal number m. As in the case of no magnetic field (NVC), the growth rate has a maximum at some intermediate value of m. Using our parameters, the disk with a strong magnetic field ($\beta^{-1} = 1$) has a fastest growing mode with $|w_I| \sim 0.48\Omega_D$ at $m \sim 11$. This corresponds to a growth time of order 10^3 yr, much smaller than the usual evolution timescale of the protostellar or the protoplanetary disk ($\sim 10^6$ yr) (Adams et al.

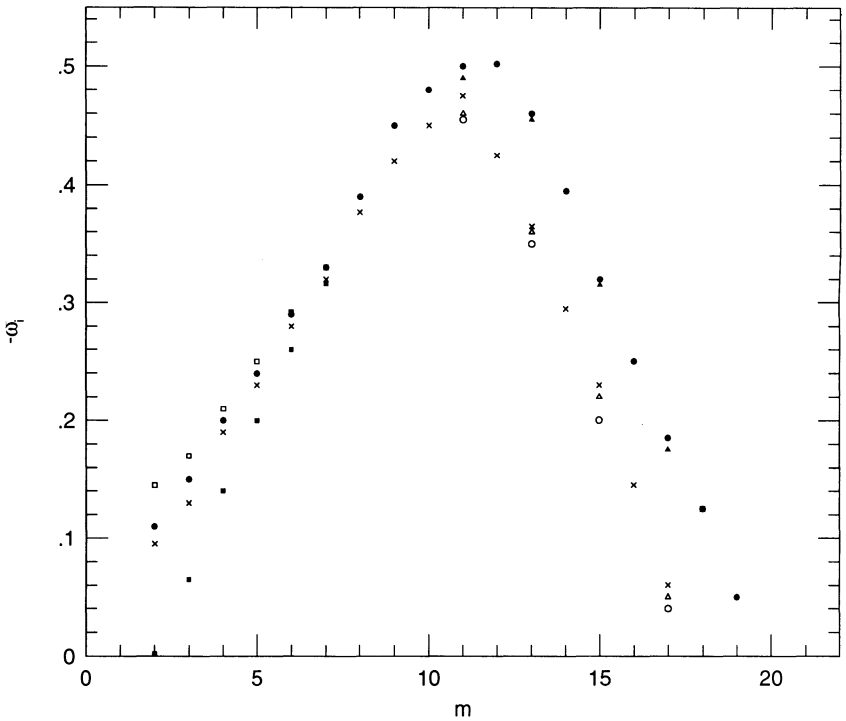

FIG. 1.—Growth rates ($\equiv -w_I$) in units of Ω_D are plotted as a function of an azimuthal number m. The different inner BCs (transmitting, reflecting) and outer BCs (zero Lagrangian pressure perturbation, transmitting) are used. Filled circles show the growth rates with no magnetic field using transmitting inner BC and zero Lagrangian pressure perturbation outer BC. Filled triangles show the growth rates with magnetic field ($\beta^{-1} = 0.1$) using the same BCs as for filled circles. Crosses are the growth rates with magnetic field ($\beta^{-1} = 1$) using the same BCs as for filled circles. Open triangles are the growth rates with no magnetic field and no dust using the same BCs as for filled circles. Open circles show the growth rates with no magnetic field and with increasing gas pressure (by a factor of 2) using the same BCs as for the filled circles. Open squares are the growth rates for $\beta^{-1} = 1$ using reflecting inner BC and zero Lagrangian pressure outer BC. Filled squares are the growth rates for $\beta^{-1} = 1$ using transmitting BC for both inner and outer boundaries.

1989). As explained in NVC, at small wavenumbers the growth rate is small because the disk is dominated by shearing due to differential rotation. The disk is unstable on some intermediate scales in which the gravity dominates the thermal and magnetic pressure. At large wavenumbers, the instability is suppressed by thermal and magnetic pressures and the disk is stabilized.

We show the effect of the magnetic field on the growth rate by changing the value of β^{-1} ($\equiv$ the ratio of magnetic pressure to the gas pressure). As β^{-1} increases, the growth rate for each m becomes smaller. This is largely due to magnetic pressure. The inclusion of the magnetic field shifts the value of m_*, where the growth rate has a maximum, to a lower value. The reason is because for other parameters fixed (e.g., surface density) m_* decreases as the total pressure increases.

The effect of the magnetic field is also shown in the eigenfunctions. For each component (gn, gi, dn), the perturbed surface density as a function of the logarithmic radial distance is presented for different strength of the equilibrium magnetic field in terms of $\beta^{-1} = 0.1, 1$ (Figs. 2, 3, 4, and 5). Since this is a linear calculation, the scales of the perturbed quantities are arbitrary . Generally the eigenfunctions are oscillating and the wavelength increases as the perturbation moves to outer part of the disk. This is due to the decreasing amount of the total pressure as the radial distance increases. The perturbed magnetic fields in radial direction show very similar behavior to those in azimuthal direction (Figs. 6 and 7), although their amplitudes are very small. As we mentioned earlier, in equilibrium the radial magnetic field is assumed to be much smaller than the azimuthal magnetic field, and its contribution to the instability is almost negligible.

For a different value of β^{-1}, we can compare the behavior of the eigenfunctions for three different components. The neutral gas and dust change only slightly with the magnetic field. Both of these components interact indirectly with the magnetic field through the collisions with the ionized gas component. On the other hand, the ionized gas component (Figs. 3 and 4) which interacts directly with the magnetic field is affected substantially by the magnetic field. In a differentially rotating disk, the azimuthal magnetic field resists the shearing which would otherwise limit the growth of the perturbation. This results in the enhancement of the surface density of the matter which moves along the magnetic field (mostly in the azimuthal direction). This effect appears to be sensitive to the strength of shearing (Elmegreen 1987).

For the same value of β^{-1}, the neutral gas component shows very similar behavior to the dust component in most regions of the disk. However, near the inner the boundary of the disk, there appears some difference in phase and amplitude. This is due to our assumption that the dust has no thermal pressure, and pressure effects are important in the inner part of the disk.

The presence of a magnetic field also changes the number of radial nodes in the eigenfunctions. With the other parameters fixed, the number of radial nodes decreases slightly as the strength of the magnetic field increases because of the increased magnetic pressure (e.g., Figs. 3 and 4).

In order to see more details of the magnetic effect, we show the growth rates (open circles in Fig. 1) in which the magnetic

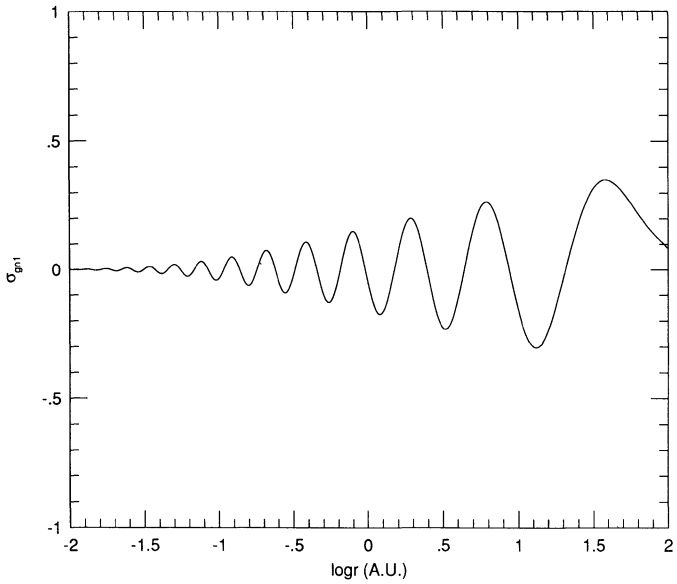

FIG. 2.—Real part of the dimensionless perturbed surface density of neutral gas is shown as a function of log r for $\beta^{-1} = 1$ and $m = 11$. The real and imaginary eigenvalues are (9.6, −0.48) in the unit of Ωp.

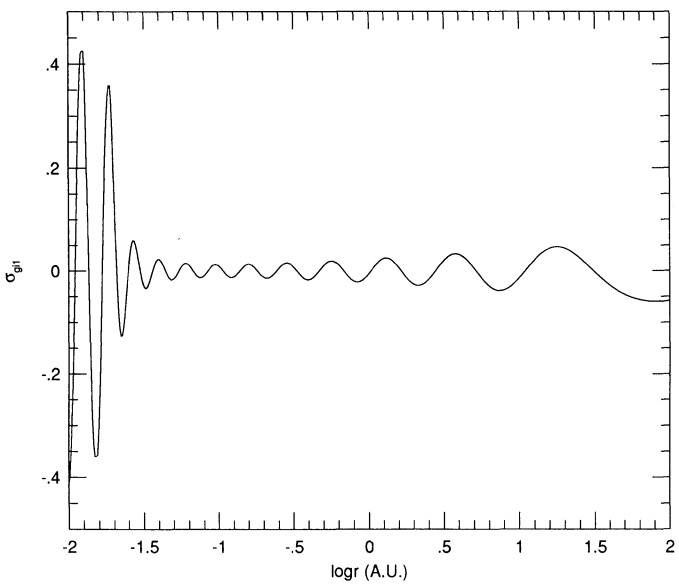

FIG. 4.—Real part of the dimensionless perturbed surface density of ionized gas is shown as a function of log r for $\beta^{-1} = 1$ and $m = 11$.

field is removed with the fixed amount of total pressure ($\sim v_A^2 + c_s^2$) for $\beta^{-1} = 1$, i.e., the gas pressure increases by a factor of 2, where $v_A \equiv B_0/\sqrt{4\pi\rho_0}$ is the Alfvén speed. Then, as shown in Figure 1, the growth rates with no magnetic field (*open circles*) are somewhat smaller than those with magnetic field for $\beta^{-1} = 1$ (*crosses*) for each m. This result shows that the magnetic field enhances the instability somewhat due to magnetic tension [$=(\boldsymbol{B}\cdot\nabla)\boldsymbol{B}/4\pi$] as well as suppressing the instability due to its pressure ($=\nabla|\boldsymbol{B}|^2/8\pi$). However, the effect of tension is much smaller than the pressure effect, so the total growth rates are reduced. This result is in agreement with the work of Elmegreen (1987), who found that for a strongly shearing environment the destabilizing effect of the magnetic field tension was more balanced by the effect of magnetic pressure.

We note that the difference between the open circles and the crosses increases as m becomes larger, i.e., the destabilizing effects of magnetic tension are mostly seen at large m.

For small m modes, the eigenfunctions are similar to those of high m modes, i.e., they are oscillating in the radial direction and the wavelengths increase with increasing radial distance. But the number of radial nodes is smaller due to the small value of the real component of the eigenvalue w_R. As in NVC, w_R is a slowly increasing function of m.

The effect of BC is also shown in Figure 1. We fix the outer BC as $\Delta p_{tot} = 0$. As shown in NVC, the effect of the boundary condition appears only for small m modes, and the growth rates using a reflecting inner BC are larger than those using a transmitting inner BC. For a transmitting BC, as we men-

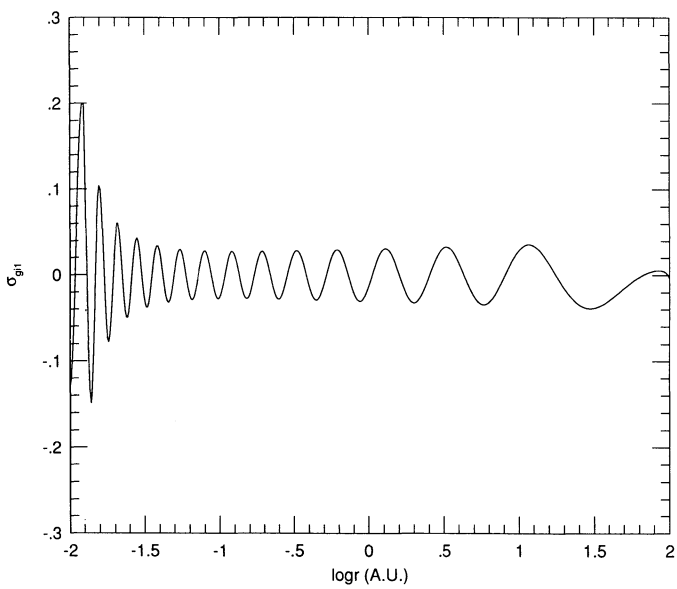

FIG. 3.—Real part of the dimensionless perturbed surface density of ionized gas is shown as a function of log r for $\beta^{-1} = 0.1$ and $m = 11$.

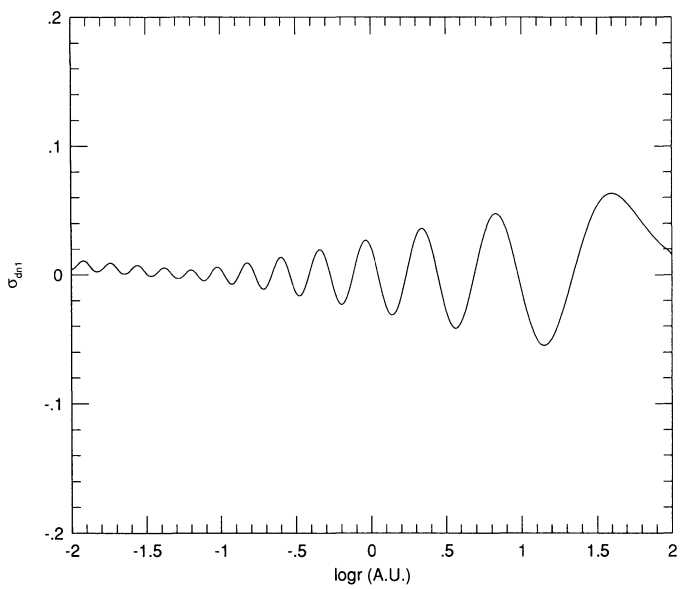

FIG. 5.—Real part of the dimensionless perturbed surface density of neutral dust is shown as a function of log r for $\beta^{-1} = 1$ and $m = 11$.

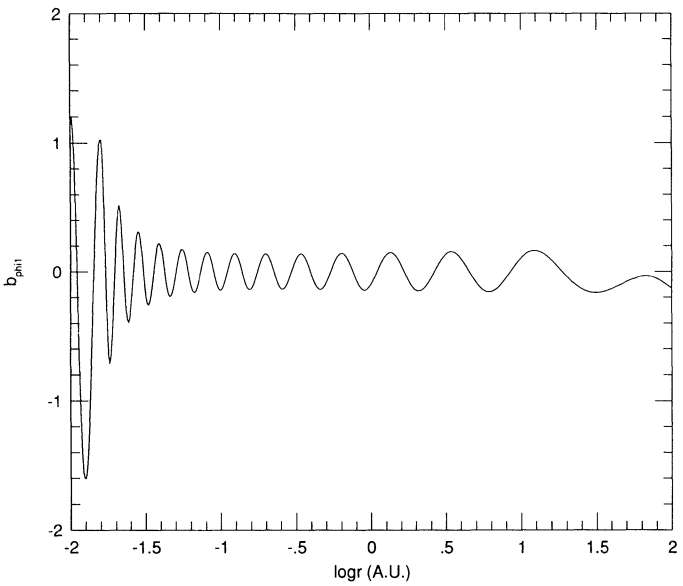

FIG. 6.—Real part of the dimensionless perturbed azimuthal magnetic field is shown as a function of log r for $\beta^{-1} = 0.1$ and $m = 11$.

tioned earlier, the wavenumber $|k|$ is obtained numerically by measuring the wavelength near inner boundary. For high m modes, the corresponding wavelength is very small, so much better numerical resolution is required. But, as we show in Figure 1, the effect of the BC appears only for small m modes. Then the small error due to the numerical resolution does not noticeably affect the results of high m modes. Using a transmitting BC for both the inner and outer boundaries reduces the growth rates significantly for small m modes, as was shown in NVC. Even for the $m = 1$ mode, the instability almost disappears by using transmitting BC at both the inner and outer boundaries. Therefore the BC effect, especially the outer BC is important to determine the instability for small m modes. More careful treatment of the BC problem is one of our future projects.

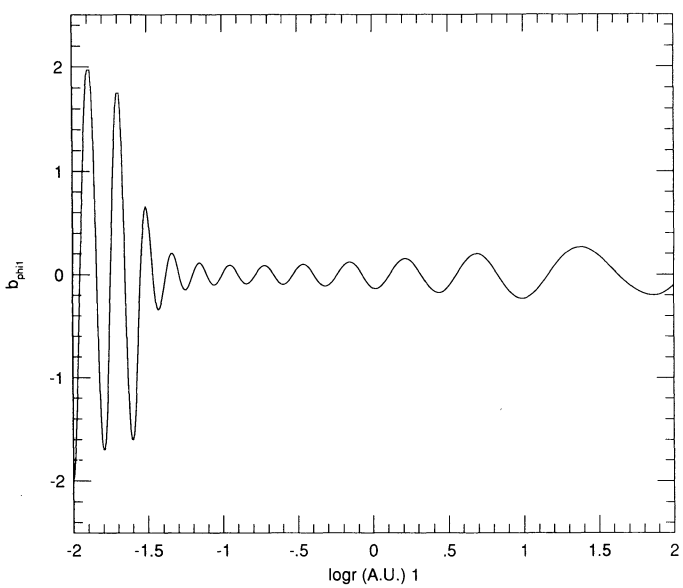

FIG. 7.—Real part of the dimensionless perturbed azimuthal magnetic field is shown as a function of log r for $\beta^{-1} = 1$ and $m = 11$.

The mass of the disk is also important in determining the disk instability as it was stressed in NVC. The magnetic effect on the growth rate appears similarly for a small disk mass ($0.1\ M_\odot$) in which $\beta^{-1} = 1$ (Fig. 8). The growth rates of the same disk mass without magnetic field are compared (filled ones in Fig. 8). For $m = 1$ mode, we include "indirect potential" induced by the separation between the central star and the center of the mass of the system (Adams et al. 1989). For $\beta^{-1} = 1$ the instability of a disk with mass $0.1\ M_\odot$ almost disappears for almost all of m except $m = 1$ and a few small values of m. As we show, the magnetic effect is important on small scales, and the $m = 1$ mode is not affected much by the magnetic field.

The ionization fraction $x \equiv \sigma_{gi0}/\sigma_{gn0}$ is one of the important factors affecting the instability, because a large value of x corresponds to strong coupling between the magnetic field and the neutral gas. The effect of x on the gravitational instability was previously studied by Langer (1978) for the case of axisymmetric perturbations in an isothermal interstellar cloud with no rotation, uniform density and magnetic field. Our result shows that different values of x do not change the main features of the growth rate, i.e., the maximum instability occurs at the same value of m (Fig. 9). But increasing the value of x somewhat reduces the growth rates, and this effect appears more clearly on small scales. For very small values of x, a decoupling between the neutral gas and the magnetic field might occur, i.e., the ionized component and the magnetic field may slip past the neutral components (Mestel & Spitzer 1956; Spitzer 1962, 1968; Langer 1978). In our model, a small values of x ($\sim 10^{-11}$) makes the system slightly more unstable than a disk with $x = 10^{-10}$ on small and intermediate scales, and there is almost no difference in the growth rates on large scales.

In this paper, we assume that the ohmic dissipation is negligible. The timescale of the ohmic dissipation turns out to be proportional to the square of the characteristic length of the magnetic field when the conductivity is constant. The ratio of the ohmic dissipation timescale to the Keplerian period ($=2\pi/\Omega$) can give some idea of the importance of the magnetic field, i.e., if the ohmic dissipation timescale is much larger than the Keplerian period, the magnetic field is almost frozen to the gas and the field may be amplified due to the differential rotation of the disk (Umebayashi & Nakano 1988). Assuming that the scale of the magnetic field is comparable to the half thickness of the disk, this ratio was calculated as a function of disk radius, which shows that the magnetic field turns out to be coupled to the gas strongly at $r \geq 15$ AU (for $\sigma_{g0}/\sigma_{d0} = 1$), and at $r \geq 2$ AU (for $\sigma_{g0}/\sigma_{d0} = 10^4$).

The instability is also somewhat sensitive to the strength of the friction. In Figure 10, we show the effect of friction on the growth rate for a different value of friction coefficient A which depends on the collision timescales between each component. In all cases, we fix the magnetic field strength as $\beta^{-1} = 1$. As shown in NVC, a large A decreases the growth rate. However, decreasing A by a factor of 0.1 does not change the growth rates much. Therefore, the growth rates are almost saturated as the friction term decreases further. The effect of friction also appears to be large on small scales.

The inclusion of dust enhances the instability because we assume thermal pressure is negligible for dust. However, for a strong magnetic field (e.g., $\beta^{-1} = 1$), this effect is weakened because the magnetic pressure acts on the dust through the collisions with ionized gas. Therefore, growth rates with dust and a magnetic field of $\beta^{-1} = 1$ are slightly larger than those

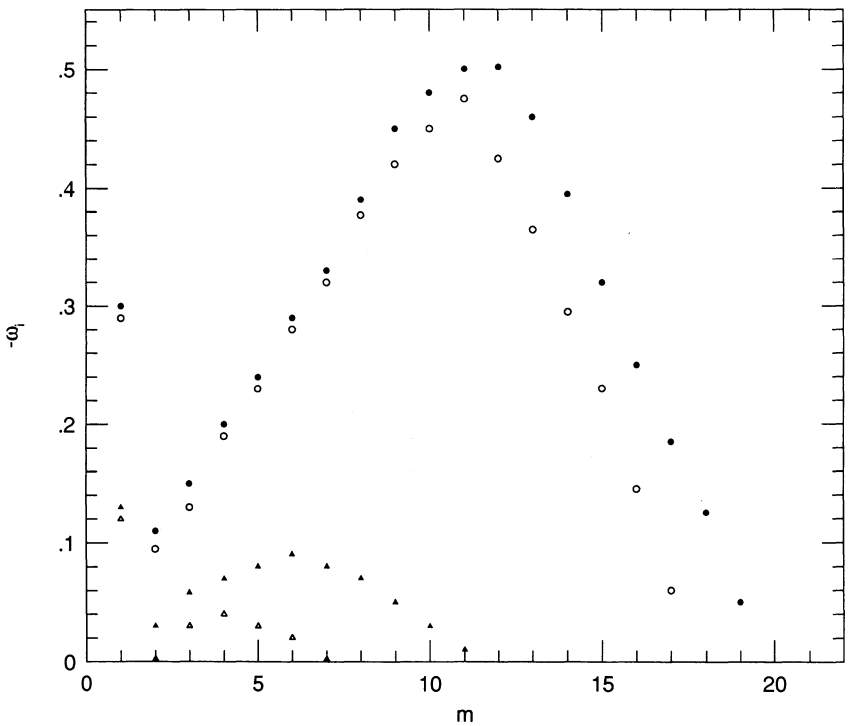

FIG. 8.—Growth rates as a function of m are shown for disk mass 0.5 $M_\odot$ with no magnetic field (*filled circles*), with magnetic field of $\beta^{-1} = 1$ (*open circles*), and 0.1 $M_\odot$ with no magnetic field (*filled triangles*), with magnetic field of $\beta^{-1} = 1$ (*open triangles*).

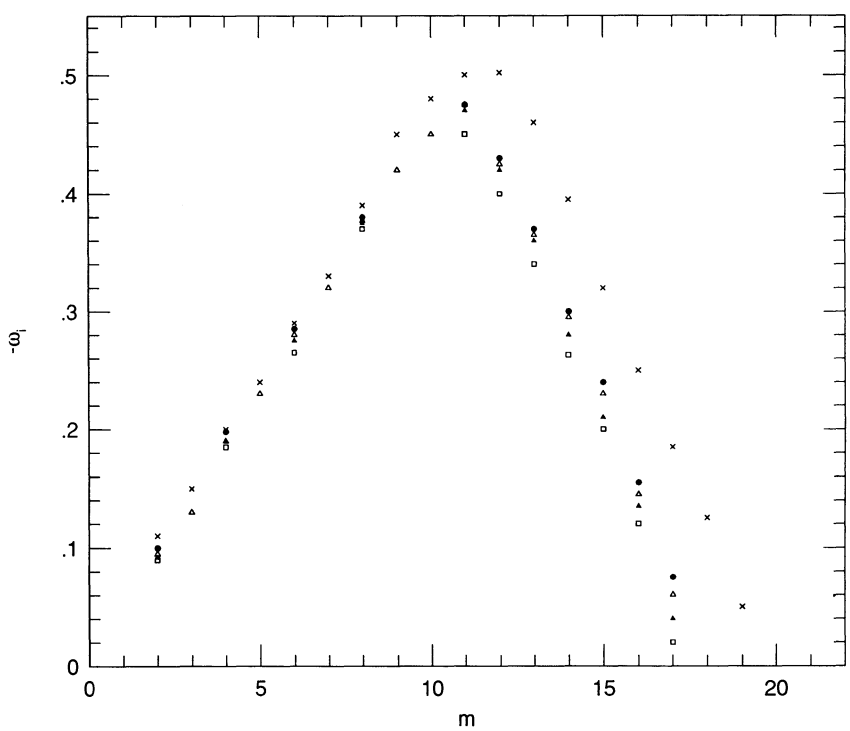

FIG. 9.—Growth rates as a function of m are shown for no magnetic field (*crosses*), $x = 10^{-11}$ (*filled circles*), 10^{-10} (*open triangles*), 10^{-9} (*filled triangles*) and 10^{-8} (*open squares*). For all cases, $\beta^{-1} = 1$, $m_d = 0.5\ M_\odot$.

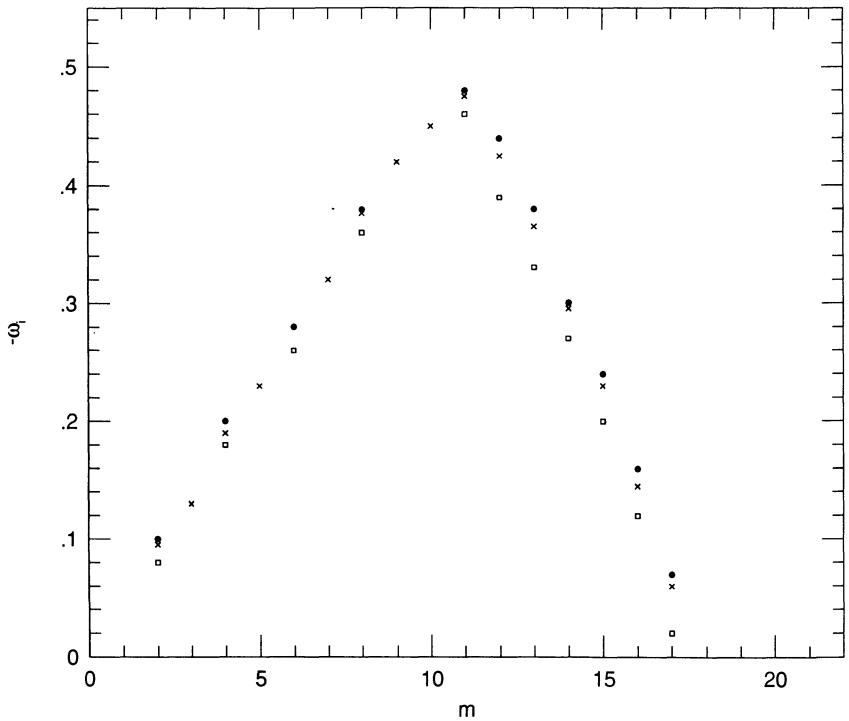

FIG. 10.—Growth rates as a function of m for different coefficients $0.1A$ (*filled circles*), A (*crosses*), $10A$ (*open squares*). For all cases, $\beta^{-1} = 1, m_d = 0.5\ M_\odot$.

with no magnetic field and no dust (open triangles in Fig. 1), especially for the high m modes in which the magnetic effect is important.

In conclusion, we have shown that a Keplerian protoplanetary disk with a magnetic field is gravitationally unstable to nonaxisymmetric linear perturbations for some range of the azimuthal number m. The magnetic field generally suppresses the instability due to its pressure, although the magnetic tension increases the growth rates slightly. This effect is shown more strongly for high m modes. The value of m at which the growth rate has a maximum becomes a little lower as the magnetic field is stronger. The enhancement of the growth rates by the inclusion of dust is somewhat reduced due to the magnetic pressure which also affects the dust indirectly through friction with the ionized gas. The effect of the ionization abundance and friction on the growth rates are also shown. We have shown the effect of the boundary conditions on instability using two different boundary conditions, the reflecting and the transmitting boundary, and it appears to be important only for small m modes.

This work was supported in part by NASA grant NAGW 2418.

REFERENCES

Adams, F. C., Ruden, S. P., & Shu, F. H. 1989, ApJ, 347, 959
Aumann, H. H., et al. 1984, ApJ, 278, L23
Bertout, C., Basri, G., & Bouvier, J. 1988, ApJ, 330, 350
Elmegreen, B. G. 1979, ApJ, 232, 729
———. 1987, ApJ, 312, 626
Langer, W. D. 1978, ApJ, 225, 95
Larson, R. B. 1984, MNRAS, 206, 197
Lee, T., Papanastassiou, D. A., & Wasserburg, G. J. 1977, ApJ, 211, L107
Levy, E. H., & Sonett, C. P. 1978, in Protostars and Planets, ed. T. Gehrels (Tucson: Univ. Arizona Press), 516
Mestel, L., & Spitzer, L., Jr. 1956, MNRAS, 116, 583
Noh, H., Vishniac, E. T., & Cochran, W. D. 1991, ApJ, 383, 372 (NVC)
Papaloizou, J. C. B., & Lin, D. N. C. 1989, ApJ, 344, 645
Shu, F. H., Tremaine, S., Adams, F. C., & Ruden, S. P. 1990, ApJ, 358, 495
Spitzer, L., Jr. 1962, Physics of Fully Ionized Gases (New York: Interscience)
———. 1968, Diffuse Matter in Space (New York: Interscience)
———. 1978, Physical Processes in the Interstellar Medium (New York: Wiley)
Strom, K. M., Strom, S. E., Edwards, S., Cabrit, S., & Skrutskiei, M. F. 1989, AJ, 97, 1451
Umebayashi, T. 1983, Prog. Theor. Phys., 69, 480
Umebayashi, T., & Nakano, T. 1988, Prog. Theor. Phys. Suppl., 96, 151